

## An analysis of GAME and SKYNET radiation data sets (Session 1: Radiation studies)

|                              |   |
|------------------------------|---|
| 著者                           | KIM Do-Hyeong, NAKAJIMA T., TAKAMURA T., Sohn B. J., TAKEUCHI N., HASHIZUME M., CHABANGBOM A.   |
| journal or publication title | Bulletin of the Terrestrial Environment Research Center, the University of Tsukuba, Proceedings of the International Workshop on GAME-AAN/Radiation |
| volume                       | 1   |
| number                       | 分冊  |
| page range                   | 5-8   |
| year                         | 2001-03   |
| URL                          | <a href="http://doi.org/10.15068/00147152">http://doi.org/10.15068/00147152</a>   |

# An analysis of GAME and SKYNET radiation data sets

Do-Hyeong Kim<sup>1</sup>, T. Nakajima<sup>2</sup>, T. Takamura<sup>3</sup>, B. J. Sohn<sup>1</sup>, N. Takeuchi<sup>3</sup>, M. Hashizume<sup>4</sup>, and A. Chabangborn<sup>5</sup>

School of Earth and Environmental Sciences, Seoul National University<sup>1</sup>,  
Center for Climate System Research, University of Tokyo<sup>2</sup>,  
Center for Environmental Remote Sensing, Chiba University<sup>3</sup>,  
Department of Geology Faculty of Science, Chulalongkorn University<sup>4</sup>

## 1. INTRODUCTION

The importance of the anthropogenic aerosols has been becoming apparent in a radiative influence on climate. This anthropogenic aerosol produces a radiative forcing of roughly  $-2 \text{ Wm}^{-2}$  that is comparable to that of greenhouse gases through the direct and indirect effects (Charlson et al., 1992). Kiehl and Briegleb (1993) showed anthropogenic sulfate aerosols contribute a globally averaged annual forcing of  $-0.3 \text{ Wm}^{-2}$ . But the aerosol optical characteristics are different from geographical and seasonal distributions, so there is large uncertainty in evaluating radiative forcing of anthropogenic aerosol.

A surface measurement network as part of the GAME AAN scientific activities to study a role of the Eurasian continent in the climate system provides the long-term period data. This data include the surface solar radiation, so in this study we will analyze and discuss the temporal and spatial difference of aerosol optical characteristics.

## 2. GROUND MEASUREMENTS OF SOLAR RADIATION

The solar radiation data at GAME site of Si-Samrong (17.17°N, 99.87°E) in Thailand and Mandalgovi (45.59°N, 106.19°E), Dunhuang (40.16°N, 94.80°E), Hefei (31.90°N, 117.16°E), Shouxian (32.55°N, 116.78°E), Yinchuan (38.48°N, 106.22°E), in China measured from 1997 to 2000 are analyzed in order to characterize the regional background aerosol optical properties and surface radiation budget. And the data at the background atmosphere-monitoring site (36.52°N, 126.32°E) in Anmyon-Do, which is located on the west coast of the Korean peninsula measured from 15 March 2000 to 30 April 2000, are also analyzed.

Both sky radiance and solar radiative flux

measurements are carried out simultaneously, but among the experiment data of China, measurements of direct and diffuse solar radiative flux aren't carried out in Mandalgovi, Dunhuang, and Yinchuan.

### 1) Sky radiometer data

The sky radiometer was used for measuring sky radiation in the solar aureole region at the wavelength of 315, 400, 500, 675, 870, 940, and 1020 nm. The measurements are carried out with the sky radiometer pointed along a conical surface with the same zenith angle of the Sun (almucantar) from 0° to 160°.

The measured direct and diffuse solar radiance data are analyzed by applying the SKYRAD.pack code developed by Nakajima et al. (1996b) for the retrieval of aerosol optical thickness, size distribution, single-scattering phase function and complex refractive index. The aerosol optical thickness  $\tau_{a\lambda}$  has been determined by subtracting optical thickness by Rayleigh scattering ( $\tau_{m\lambda}$ ) and by ozone absorption ( $\tau_{o\lambda}$ ) as

$$\tau_{a\lambda} = \frac{\ln(F_{o\lambda} / F_{\lambda})}{m} - \tau_{m\lambda} - \tau_{o\lambda} \quad (1)$$

where  $F_{o\lambda}$  is the direct solar radiation assumed to be at the top of the atmosphere and  $F_{\lambda}$  is the measured direct solar irradiance at the ground. Relative optical air mass  $m$  is obtained by the inverse of cosine of the solar zenith angle.  $\tau_{m\lambda}$  is the optical thickness of by Rayleigh scattering and  $\tau_{o\lambda}$  is the ozone optical thickness. The calibration coefficient  $F_{o\lambda}$  is obtained by improved Langley method, which gives a better correlation coefficient.

### 2) Solar radiative flux data

Pyranometer were used for measuring the total downward solar flux and diffused solar radiative flux by the solar occultation method in the wavelength region between 0.3 and 2.8  $\mu\text{m}$ . The direct solar radiative flux is also measured by pyheliometer. This pyheliometer measures

the intensity of a radiant beam at normal incidence that comes only from the solar disk, which includes about 5 deg. of circumsolar radiation.

### 3. RESULTS

#### 1) Analyses of the sky radiometer data

Monthly and daily averaged aerosol optical thickness (AOT) at 500 nm for the 3 different observation sites is presented in Fig. 1. Optical thickness of the three sites show different pattern although their measurement periods aren't exactly the same. The averaged value of the Dunhuang (DH) and Si-Samrong (SS) is 0.336, 0.503 each other, the maximum is shown in March or April and minimum, Oct and Nov in both sites. This can be derived by seasonal variation in concentration of aerosol particles.

In the case of Anmyon-Do (AM) averaged value is 0.583, but sometimes we can see very large value reached 2.0 and  $\alpha$  defined by eq. (2) is as small as 0.1 at the same time. This period is coincident with Yellow Sand (Asian dust) event (Korean Meteorological Administration, 2000), which is heavy dust originated from the desert areas of North China, in particular, during the springtime.

In order to examine the optical characteristics as a function of wavelength dependence of optical thickness we present the Ångström exponent  $\alpha$

$$\tau_{a\lambda} = \tau_{0.5} \left( \frac{\lambda}{0.5} \right)^{-\alpha} \quad (2)$$

where  $\lambda$ 's are wavelengths of the sky radiometer. We show the scatterplot of  $\tau_{0.5}$  versus  $\alpha$  in Fig. 2. Ångström exponent present the characteristics of their base aerosol properties more efficiently, the averaged value shows distinguished difference between SS and DH as 1.350 and 0.285. This means the concentration of particle size distribution, that is, the main component of the particles in SS is composed of submicron particles, and DH, sand dust like particles. DH shows the negative correlation between  $\tau_{0.5}$  and  $\alpha$ . Kaufman et al. (1994) showed the desert transition zone has the negative correlation and Nakajima et al. (1989) showed this can be explain by growing aerosol particles by prevailing soil-derived particles. In AM various size of the aerosol exists, whose range of the  $\alpha$  is from 0.2 to 1.5 when AOT is within 0.5, AOT increases as the large particle concentration increases.

Fig. 3 shows columnar aerosol volume spectra at three sites in different time. The obtained spectra distributions of base aerosol indicate a two-modal pattern but mode radius and volume distributions show different pattern as season.

As expected,  $\alpha$  increases with an increase in concentration of small particles, at the same time, decrease in that of large particles. AOT increases with increase of small particles at SS, on the other hand, with increase of large particles at DH. The volume spectra in yellow sand event show significant increase of large particles, simultaneous with decrease of small particles, with new peak at around 2 - 4  $\mu\text{m}$ .

#### 2) Analysis of the solar radiative flux data

The absolute value of imaginary part of the aerosol refractive index (absorption index) is extracted from the direct and diffuse solar radiative fluxes integrated over wavelengths from 0.3 to 2.8  $\mu\text{m}$  using the radiative transfer model (rstar5b) developed by Nakajima et al. (1988). For the calculation we used the measured aerosol optical thickness and size distribution by SKYRAD.pack. The Absorption index is determined from comparison of theoretical and measured values of flux.

Retrieved absorption index is presented in Fig. 4 with the values from SKYRAD.pack. Most of retrieved absorption indices range from 0.005 to 0.01 in AM, and around 0.01 in SS. As comparison with aerosol optical thickness, the retrieved values of the aerosol absorption index decreases when the AOT increases, as shown by Nakajima et al. (1996a). As for the yellow sand case of April 7, the retrieved absorption index indicates as large as 0.003.

### 4. REFERENCES

- Charlson, R. J., S. E. Schwartz, J. M. Hales, R. D. Cess, J. A. Coakley Jr., J. E. Hansen, and D. J. Hofmann, 1992: Climate forcing by anthropogenic aerosols. *Science*, **255**, 423-430.
- Kaufman, Y. J., A. Gitelson, A. Karnieli, E. Ganor, R. S. Fraser, T. Nakajima, S. Mattoo, and B. N. Holben, 1994: *J. Geophys. Res.*, **99**, 10341-10356.
- Kiehl, J. T., and B. P. Briegleb, 1993: The relative roles of sulfate aerosols and greenhouse gases in climate forcing. *Science*, **260**, 311-314.

- Nakajima, T and M. Tanaka, 1988: Algorithms for radiative intensity calculations in moderately thick atmospheres using a truncation approximation, *J. Quant. Spectrosc. Radiat. Transfer*, **40**, 51-69.
- Nakajima, T. M. Yamano, M. Shinobara, K. Arai, and Y. Nakanishi, 1989: Aerosol optical characteristics in the yellow sand events observed in May 1982 in Nagasaki -- Part II Model. *J. Meteor. Soc. Japan*, **67**, 279-291.
- Nakajima, T., T. Hayasaka, A. Higurashi, G. Hashida, N. Mohorram-Nejad, Y. Najafi, and H. Valavi, 1996a: Aerosol optical properties in the Iranian region obtained by ground-based solar radiation measurements in the summer of 1991. *J. Appl. Meteorol.*, **35**, 1265-1278.
- Nakajima, T., G. Tonna, R. Rao, R. Boi, Y. Kaufman, and B. Holben, 1996b: Use of sky brightness measurements from ground for remote sensing of particulate polydispersions, *Applied Optics*, **35**, 2672-2686.
- Nakajima, T. and A. Higurashi, 1997: AVHRR remote sensing of aerosol optical properties in the Persian Gulf region, summer 1991. *J. Geophys. Res.*, **102**, 16935-16946.

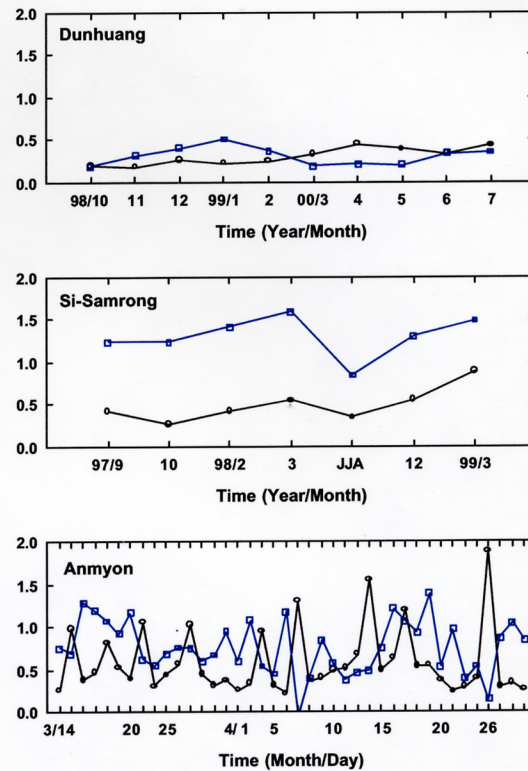


Fig. 1: Monthly (Dunhuang, Si-Samrong) and daily (Anmyon-Do) averaged values of Ångström exponent (thin line and square) and aerosol optical thickness (thick solid line and circle) at 500 nm.

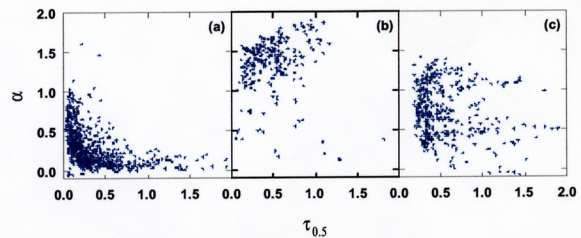


Fig. 2: Scatterplot of the Ångström exponent versus aerosol optical thickness at the wavelength of 500 nm. (a) Dunhuang, (b) Si-Samrong, (c) Anmyon-Do.

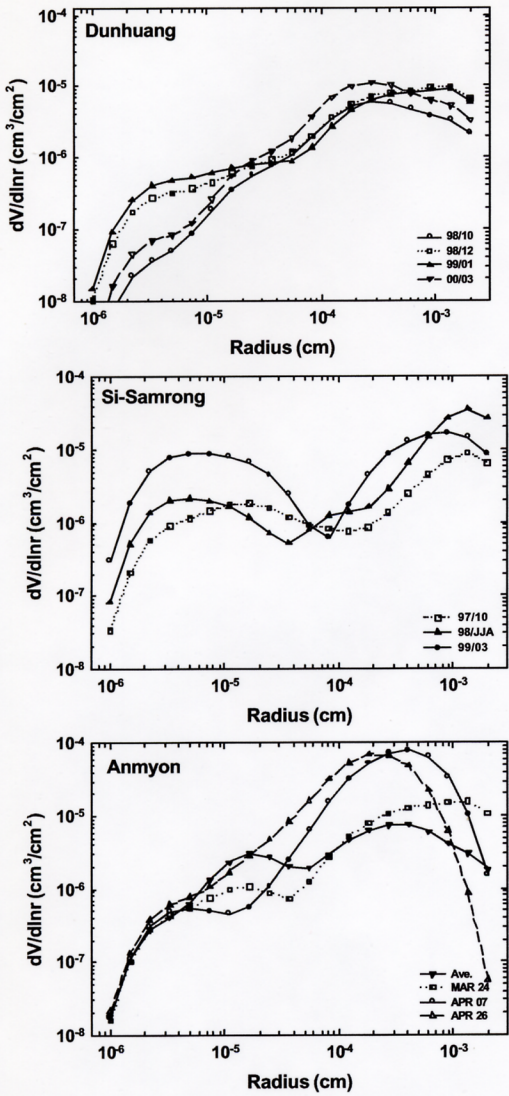


Fig. 3: Aerosol volume spectra of Dunhuang, Si-Samrong and Anmyon-Do (Cases of March 24, April 7 and 26, 2000 correspond to the yellow sand events).

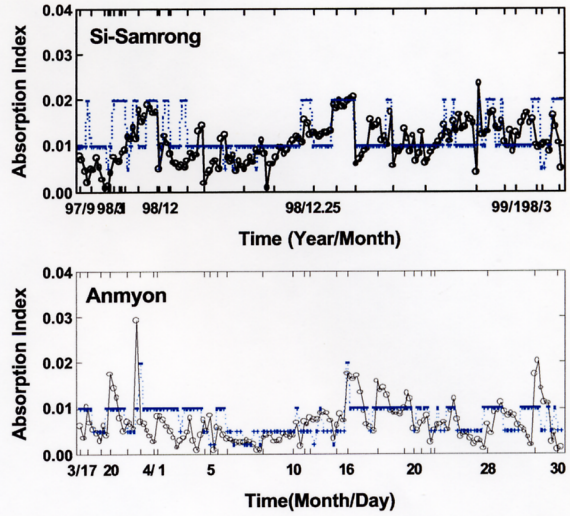


Fig. 4: Time series of retrieved value of imaginary part of refractive index (thick solid line and circle) and retrieved values from SKYRAD.pack.